g-C_3N_4/TiO_2 NANOCOMPOSITES AND THEIR APPLICATION IN PHOTOCATALYTIC CO_2 REDUCTION: A MINIREVIEW

M. MANRIQUE-HOLGUÍN, J.J. ALVEAR-DAZA,
J.A. RENGIFO-HERRERA and L.R. PIZZIO

Laboratory of Advanced Oxidation Processes and Photocatalysis (LAPh), Centro de Investigación en Ciencias Aplicadas "Dr. Jorge J. Ronco" (CINDECA) (CCT La Plata CONICET, UNLP, CICPBA), Departamento de Química, Facultad de Ciencias Exactas, Universidad Nacional de La Plata, 47 No. 257, La Plata, Argentina
lrpizzio@quimica.unlp.edu.ar; julianregifo@quimica.unlp.edu.ar

***Abstract*— g-C_3N_4/TiO_2 nanocomposites seem to be promising materials for photocatalytic reductive applications such as water splitting and CO_2 reduction. The g-C_3N_4 is known as a metal-free semiconductor exhibiting a high reductive conduction band (CB) (-1.3 V vs. NHE) and visible light absorption (E_g =2.7 eV), while TiO_2 is the most popular photocatalyst. However, both semiconductors show high electron/hole recombination, and in the case of TiO_2, lack of visible light absorption. Both problems could be overcome by designing type II heterojunctions or a direct Z-scheme between g-C_3N_4 and TiO_2. These strategies make these composites suitable for CO_2 photocatalytic reduction and solar fuel production. Herein, the main aspects related to photocatalytic CO_2 reduction in aqueous media to obtain solar fuels such as methane and methanol, synthesis of g-C_3N_4/TiO_2 nanocomposites, and their reactivity will be addressed and reviewed.**

***Keywords*— g-C_3N_4, TiO_2, heterojunctions, direct Z-scheme, CO_2 reduction, solar fuels**

I. INTRODUCTION

The presence of greenhouse gases such as CO_2, methane (CH_4), fluorinated gases, and NO_x on the planet´s atmosphere causes a detrimental effect on the global climate (global warming). Data from the US Environmental Protection Agency (USEPA) revealed that CO_2 accounts for 80% of the total greenhouse gas emissions from the combustion of nonrenewable energy sources (oil derivatives and charcoal) (US Environmental Protection Agency, 2022). Between 2001 and 2014, the World Bank reported a rise of CO_2 emissions at global scale from 22 to 36 million kt, while in 2016 Argentina's CO_2 emissions amounted to around 200.000 kt (Banco Mundial, 2022).

Due to the above, the interest in reducing CO_2 emissions has been steadily increasing, and one of the strategies is the production of chemical compounds from CO_2. Heterogeneous catalytic processes such as heterogeneous photocatalysis, heterogeneous electrocatalysis, and heterogeneous photoelectrocatalysis exhibit interesting features to convert CO_2 into solar fuels such as CH_4 and CH_3OH (Tu *et al.*,2014; Xie *et al.*, 2021). Applications of TiO_2 based photocatalytic technologies have been historically addressed to employ the oxidant capacity of photoinduced valence band holes (h^+_{VB}) to remove organic pollutants and bacteria from water and air.

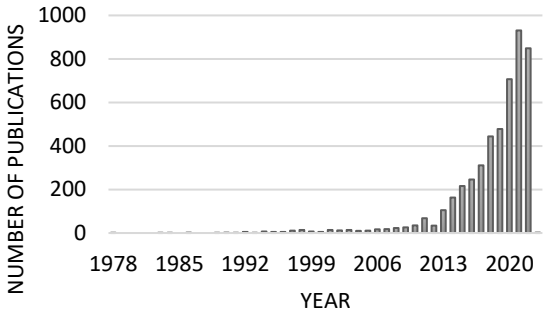

Figure 1: Number of publications per year about CO_2 photoreduction by using Scopus database.

g However, the first study reporting the photocatalytic CO_2 reduction on TiO_2 nanoparticles was published in the late 70´s by Inoue *et al*. (1979). But the necessity to find novel strategies to mitigate CO_2 in the atmosphere has led to a rebirth of this technology in the last 10 years (Fig. 1).

TiO_2 would mimic the process occurring in a plant leaf through photosynthesis, where CO_2 molecules are captured and then converted into more complex substances via several photoinduced reactions (Abdullah *et al.*, 2017). The photocatalytic CO_2 reduction shows another interesting feature besides the production of solar fuels: the possibility to use solar light, a renewable energy source, to excite the photocatalyst. However, TiO_2 nanoparticles do not exhibit visible light absorption since their band gap energy (E_g) is around 3.2 eV, allowing only UV wavelengths, less abundant on the planet´s surface (4%-7%), to photoinduce charge carriers. This fact makes the development of visible-light TiO_2 nanomaterials, which are able to take better advantage of more abundant wavelengths such as visible light (50%), an attractive strategy to overcome this drawback.

Graphitic carbon nitride (g-C_3N_4), a metal-free semiconductor with visible light absorption (E_g= 2.7 eV), has a conduction band redox potential able to reduce CO_2 molecules, but a high electron-hole recombination and low specific surface area limit its use as photocatalyst in these applications. Nevertheless, heterojunctions between TiO_2 and g-C_3N_4 seem to be an attractive strategy to overcome the lack of visible light absorption of TiO_2 and the limitations of g-C_3N_4 mentioned above (Wen *et al.*, 2017).

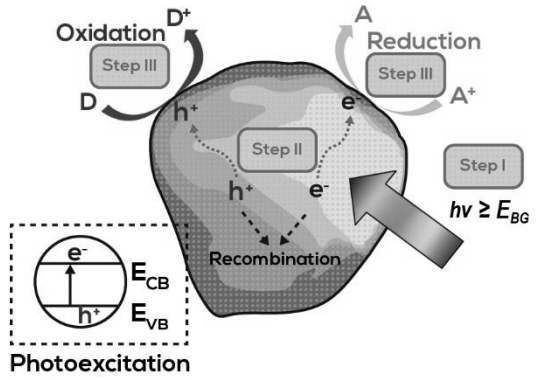

Figure 2: Primary events occurring in illuminated TiO_2 nanoparticles.

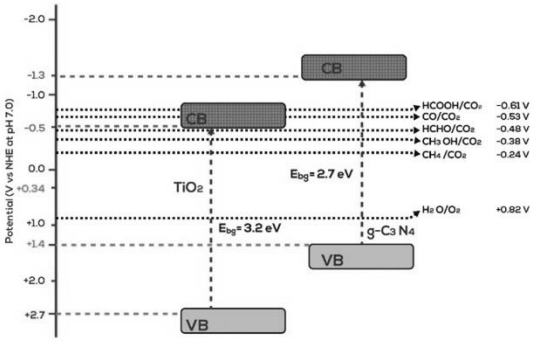

Figure 3: Redox potentials of CO_2 reduction vs. semiconductor band positions.

This minireview is devoted to showing the main aspects linked to the photocatalytic reduction of CO_2 and its conversion into solar fuels by using visible-light active g-C_3N_4/TiO_2 composites.

II. PRIMARY EVENTS OCCURING IN ILLUMINATED TiO_2 NANOPARTICLES

A. TiO_2 nanoparticles under UVA irradiation

When TiO_2 nanoparticles are irradiated by UVA light ($\lambda <$ 400 nm), whose wavelengths have enough energy to overcome their E_g, electrons (e^-) located in the valence band (VB) are promoted to the conduction band (CB), generating charge separation and inducing electron-hole pairs (this event takes place in the first nanoseconds (ns)) (Fig. 2) (Ward *et al.*, 1983).

Unfortunately, most of these charge carriers (~90%) undergo a fast recombination within the first nanoseconds, dissipating the energy excess in the form of heat (Mohamed and Bahnemann, 2012). Those charge carriers that survived from recombination can be trapped on different surface defects present on the metal oxide surface (in the scale of microseconds (μs)). For instance, electrons are mostly trapped onto pentacoordinated Ti^{4+} sites commonly named as oxygen vacancies (V_o), while photoinduced holes are trapped on Ti-OH sites. These trapped charges can react further with suitable donors and acceptors (in the scale of milliseconds (ms)) (Schneider *et al.*, 2014).

Suitable electron acceptors must have a more positive potential than that of conduction band photoinduced electrons (e^-_{CB}) (around -0.5 V vs. NHE at pH 7.0), while suitable electron donors should exhibit a more negative potential than that of photoinduced h^+_{VB} (+2.7 V vs. NHE at pH 7.0) (Zhang *et al.*, 2012; Rengifo-Herrera *et al.*, 2022) (Fig. 3).

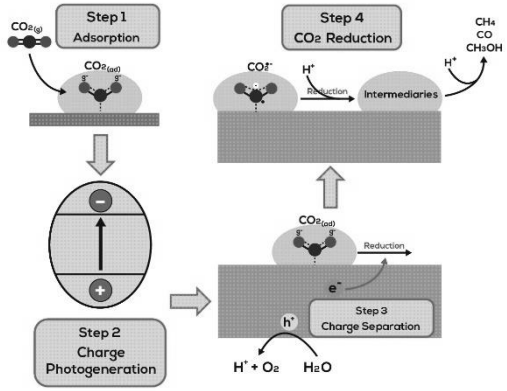

Figure 4: Steps to achieve CO_2 photoreduction on a photocatalyst.

Considering the time of each primary event occurring after UVA light irradiation, it is clear that there is a strong competition between the generation of electron-hole pairs and recombination, since both events occur in the same time scale (nanoseconds) and for this reason this is one of the main limitations of TiO_2 photocatalytic processes.

III. PHOTOCATALYTIC REDUCTION OF CO_2 IN AQUEOUS MEDIA

A. Mimicking nature

Artificial photosynthesis seeks to mimic the natural photosynthesis process carried out in a plant leaf (Remiro-Buenamañana and García, 2019). A suitable photocatalyst for CO_2 reduction must fulfill some key features such as good carbon dioxide adsorption, high pair electron-hole generation, charge-carrier separation, and CO_2 reduction (Fig. 4) (Gong *et al.*, 2022).

The initial pH solution has a relevant role in the photocatalytic CO_2 reduction. Depending on pH, both the VB and CB of TiO_2 can undergo band bending. This fact is caused by an excessive adsorption of H_3O^+ or OH^- on the TiO_2 surface, producing a magnetic field that changes the position of Fermi energy level (E_f). At acidic or alkaline pH values, the excess of positive or negative charge in the solid-liquid interface makes these bands undergo a downward or upward band bending respectively (Schneider *et al.*, 2014). For instance, in TiO_2 nanoparticles each pH increase raises the redox potential of the CB by 59 mV, making the material more reductive (Moser and Gratzel, 1983).

When CO_2 reduction is carried out in aqueous media, the pH also plays an important role because CO_2 solubility in water is low (0.48 mg L^{-1} at 25 °C). In the presence of NaOH (0.2 mol L^{-1}), the photocatalytic CO_2 reduction is enhanced, since CO_2 solubility is highest because its acidic properties and the presence of OH^- ions may serve as a strong hole scavenger (Koci *et al.*, 2009). Moreover,

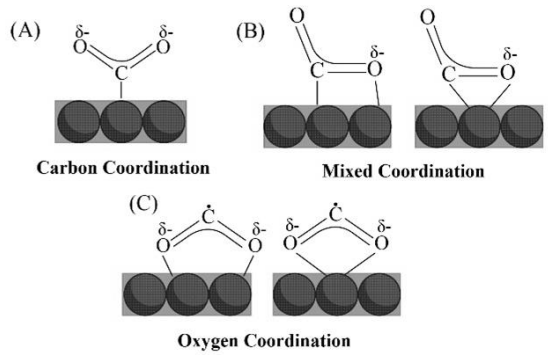

Figure 5: Types of CO_2 adsorption occurring on metal oxide semiconductors.

at alkaline pH or modifying the photocatalyst surface (adding alkaline groups to the surface), CO_2 adsorption (either as HCO_3^- or $CO_3^=$) on the photocatalyst surface is boosted (Gong *et al*., 2022). Some studies about CO_2 adsorption on TiO_2 surfaces have proposed physisorption (adsorption as a linear molecule) or chemisorption (adsorption as a partially charged species of $CO_2^{\delta\bullet-}$). This issue is key since CO_2 reduction shows a very negative redox potential (-1.9 V vs, NHE) making this process on TiO_2 or g-C_3N_4 semiconductors thermodynamically unfavorable. However, CO_2 adsorption leads to the formation of charged structures with a geometrical distortion resulting in a lower barrier for accepting electrons (Vu *et al.*, 2019). In Fig. 5, coordination schemes of CO_2 chemisorption are shown, where CO_2 or TiO_2 surface atoms behave either as Lewis acids or bases. Figure 5a shows how the O atoms of CO_2 play the role of Lewis bases, donating electron pairs to the Lewis acid centers of the photocatalyst. The opposite occurs in Fig. 5b, where the positively charged C atoms take the role of Lewis acids receiving electrons from Lewis basic centers of the photocatalysts. Moreover, Figure 5c shows a mechanism where either C or O atoms from CO_2 act as Lewis acids or bases. It is important to highlight the importance of chemisorption and the formation of $CO_2^{\delta\bullet-}$ species on the photocatalyst surface since the latter weakens the linear symmetry of CO_2 molecule (a highly stable molecule with a dissociation energy of C=O bond of around 750 KJ mol^{-1}) enhancing the production of reduced by-products. Thus, increasing the number of active sites of the photocatalyst that is able to form $CO_2^{\delta\bullet-}$ species (by chemisorption) would make CO_2 reduction more feasible.

The presence of a hole scavenger or a sacrificial electron donor (SED) is also a key factor in the photocatalytic CO_2 reduction (Shehzad *et al*., 2018). The trapping of photoinduced valence band holes by SED plays an important role since it allows a better charge separation and its oxidation produces the formation of protons that are essential to generate CO_2 reduced by-products. Often, in photocatalytic CO_2 reduction by TiO_2 materials, water is used as SED due to its abundance and low cost. However, water exhibits two important disadvantages: (i) O_2 evolution when water oxidation takes place (Fig. 3) since molecular oxygen can compete with CO_2 molecules for photoinduced conduction band electrons, and (ii) water reduction (water splitting) is thermodynamically allowed in these photocatalytic systems (E= 0.00 V compared to CO_2 reduction E= -1.90 V vs. NHE)) leading to H_2 evolution reactions (HER). These drawbacks can be overcome by a suitable photocatalyst design where reductive and oxidative sites are separated by adding co-catalysts or designing heterojunctions or Z-scheme strategies with different semiconductors. Moreover, the use of nonaqueous solvents (where CO_2 solubility can be higher than in water) or the presence of SED, such as alcohols, amines (which exhibit a higher reductive potential), benzyl-dihydronicotinamide (BNAH imitating the role of NADH in the natural photosynthesis) and ascorbic acid/thiols, can also enhance the photocatalytic CO_2 reduction.

To summarize, the overall performance of solar fuel generation by photocatalytic processes depends on the reaction medium (pH, solvent, solid/aqueous or solid/gas interfaces, etc.) the concentration of SEDs, and the photocatalyst nature. For instance, if the photocatalytic CO_2 reduction is carried out in aqueous media, the contact between CO_2 and the photocatalyst is easier to achieve than in a solid/gas interface. Moreover, in aqueous media, a high diversity of products is obtained, while in solid/gas interface it is possible to obtain CO and CH_4 only.

B. Visible-light absorbing TiO_2 based materials for CO_2 reduction

TiO_2 is a material used in different industrial applications such as cosmetics, foods, medicine, fibers, paper, resins, plastics, and paints, and its global market is estimated to be around USD 15.76 billion, making this product easily available and abundant (Parrino and Palmisano, 2021). Since the Fujishima-Honda effect was reported in the early 70s (Fujishima and Honda, 1972), when TiO_2 was used as heterogeneous photocatalyst to promote water splitting to generate H_2, its photocatalytic applications to remove chemical and biological pollution in solid/water and solid/air interfaces, for H_2 production, organic synthesis, and CO_2 reduction to produce solar fuels (CH_4 and CH_3OH) have increased in the last decades (Nahar *et al*., 2017). TiO_2 offers several advantages as photocatalyst such as abundance, physicochemical stability, and suitable conduction (-0.5 V vs. NHE) and valence (+2.7 V vs. NHE) band redox potentials able to produce highly oxidant reactive oxygen species (ROS) and e^-_{CB} with enough redox potential to reduce H_3O^+ and CO_2. Photocatalytic CO_2 reduction by-products obtained in aqueous TiO_2 suspensions or gas phase exhibit differences. For instance, the presence of water in the media leads to the formation of by-products such as CH_3OH, formic acid (COOH), and formaldehyde (CH_2O), while under gas phase the main by-products are CO and CH_4 (Nahar *et al*., 2017).

Despite these advantages, the TiO_2 photocatalyst exhibits some drawbacks linked to high electron/hole recombination and large bandgap energy, the latter limiting its use in solar applications.

There are several strategies to overcome these limitations. For instance, the modification of TiO_2 with noble

metal nanoparticles can generate Schottky barriers where photoinduced conduction band electrons can easily migrate to the metal nanoparticles, enhancing the charge carrier separation and reducing the hole/electron recombination. Moreover, the presence of noble metal nanoparticles such as silver or gold with sizes smaller than 100 nm on TiO_2 surfaces can promote localized surface plasmon resonance (LSPR), allowing the composite TiO_2/noble metal visible light absorption at wavelengths comprised between 360 and 500 nm (depending on the size of noble metal nanoparticles) (Zhang *et al*., 2013). Modification of TiO_2 surfaces with organic or inorganic dyes (photosensitization) can also confer visible light absorption. Dye may behave as an antenna absorbing visible light photons and generating excited states able to transfer electrons to the TiO_2 CB. These e^-_{CB} can participate in redox reactions in the presence of molecular oxygen and generate ROS that can destroy the organic or inorganic dye eliminating the visible light absorption of these materials (Rengifo-Herrera *et al.*, 2022).

On the other hand, there are also several reports about the use of heterojunctions or Z-scheme strategies with other metal oxides or metal-free semiconductors. Often, heterojunctions (type I or II) are carried out with other semiconductors that exhibit different positions of VB or CB than those of TiO_2. The main aim of heterojunctions is to create an intimate contact between semiconductors in order to efficiently separate the photoinduced electrons or holes, leaving the holes and electrons in the VB and CB with the highest oxidant and reductive power respectively. Thus, the literature reports the existence of type I heterojunctions where the conduction and valence bands of semiconductor 1 are respectively higher and lower than those of semiconductor 2, and type II heterojunctions where the CB and VB of semiconductor 1 are higher than those of semiconductor 2. The most common are the type II heterojunctions; however, unfortunately in this case, photoinduced h^+ remain in the VB with the less positive redox potential, while electrons are left in the most positive CB. These features negatively affect the photocatalytic performance of the nanocomposite materials (Qi *et al*., 2017).

The direct Z-scheme, which was first reported by Yu *et al*. (2013), is an interesting strategy to prepare nanocomposites of TiO_2 with other metal oxides or free-metal semiconductors. In this case, the intimate contact between semiconductors (i.e., through chemical bonds) can achieve the effective charge separation as well. The magnetic field achieved by the intimate contact between semiconductors drive electrons to the most reductive CB and holes to the most oxidative VB, generating composite materials with high photocatalytic activity.

In this regard, graphitic carbon nitride (g-C_3N_4), which is a metal-free semiconductor composed of heptazine polymeric units, offers interesting properties to be used as semiconductor in either heterojunctions or direct Z-schemes with TiO_2. Its semiconducting properties were firstly reported by Wang *et al*. (2009) and it exhibits visible light absorption (E_g = 2.7 eV) and a high reductive CB position (-1.3 V vs. NHE) (Wen *et al*., 2017). Some few studies in the literature have reported type II heterojunctions and direct Z-scheme nanocomposites between TiO_2 and g-C_3N_4 with efficient ability to reduce CO_2 into solar fuels (Adekoya *et al.*, 2017; Wang *et al.*, 2020). These g-C_3N_4 structures can be easily synthesized by thermal condensation of urea, melamine, and thiourea at temperatures beyond 400 °C. In a first stage, Urea is transformed to biuret at temperatures ranging between 300 and 350 °C, which further cyclizes to form cyanuric acid. The latter reacts with ammonia coming from urea thermal decomposition to form ammelide and subsequently, melamine. Polycondensation of melamine generates a polymer composed of melem units and finally, at temperatures around 500 °C melem undergoes high polymerization obtaining g-C_3N_4 structures (Dai *et al*., 2015).

C. Synthesis and characterization of g-C_3N_4/TiO_2 nanocomposites

There are several strategies to synthesize g-C_3N_4/TiO_2 heterojunctions such as sol-gel method, hydrothermal method, solvothermal and microwave-assisted synthesis (Acharya and Parida, 2020). However, the sol-gel synthesis has been the favorite method to obtain g-C_3N_4/TiO_2 nanocomposites. The sol-gel method is a very versatile wet synthesis where acid or base catalyzed hydrolysis of a titanium alkoxide or titanium (IV) chloride is achieved in order to obtain a gel. Parameters such as initial pH, water concentration, and organic additives allow controlling the synthesis and obtaining a material with different physicochemical properties. The obtained gel must be further annealed at temperatures beyond 400 °C to produce TiO_2 with a well-defined crystalline structure (anatase or rutile). The addition of urea, melamine or thiourea during the titanium alkoxide hydrolysis allows obtaining TiO_2/g-C_3N_4 nanocomposites, but the calcination must be carried out at temperatures of 500 °C to obtain highly polymerized g-C_3N_4 structures (Pérez-Obando *et al*., 2019).

The characterization of g-C_3N_4/TiO_2 nanocomposites requires the use of bulk and surface techniques such as X-ray diffraction (XRD), diffuse reflectance spectroscopy (DRS), X-ray photoelectron spectroscopy (XPS), surface FT-IR techniques (ATR and DRIFT), and transmission electron microscopy (TEM). A study reported by some of us revealed that the synthesis of g-C_3N_4/TiO_2 by acid catalyzed sol-gel method using urea (30% w/w) and annealing temperatures of 400 °C for 1 h produced g-C_3N_4/TiO_2 nanocomposites. XRD diffraction patterns did not show evidence of the presence of metal-free semiconductor g-C_3N_4, apparently due to its high dispersion on the TiO_2, but several peaks corresponding to TiO_2-anatase crystalline structure were found. Materials exhibited visible light absorption comprised between 400 and 500 nm, matching very well the optoelectronic properties of the metal-free semiconductor. The presence of g-C_3N_4 onto the nanocomposite was evidenced by XPS and DRIFT-FTIR measurements. N 1s and C 1s XPS signal deconvolution showed a component at 399 eV and 288

eV respectively, attributed to C=N-C bonds of heptazine rings, while the IR spectrum revealed the presence of signals in the region comprised between 1200 and 1650 cm^{-1} from the formation of extended C-N=C networks (Pérez-Obando *et al*., 2019). Most recently, we also reported the possible formation of direct Z-scheme in TiO_2 nanorods in the presence of g-C_3N_4. TiO_2 nanorods were prepared by thermal treatment of H-titanate nanotubes impregnated with urea (H-titanate:urea ratio, 1:4) and annealed at 450 °C for 1 h. In this material, unlike the previously reported, the XRD diffraction pattern showed evidence of g-C_3N_4 structures by the appearance of a peak at 27.4 ° typically assigned to this metal-free semiconductor. Moreover, by XPS a new N 1s signal at 397.5 eV was detected, probably due to the formation of Ti-N bonds. TEM micrographs also revealed an intimate contact between anatase TiO_2 and g-C_3N_4. All these findings allowed suggesting the existence of direct Z-scheme in this nanocomposite since H-titanates may show an important presence of Ti^{IV} sites allowing an interaction with formed g-C_3N_4 (through the formation of Ti-N bonds) (Osorio-Vargas *et al*., 2022).

D. Photocatalytic CO_2 reduction using g-C_3N_4/TiO_2 nanocomposites

Specific surface area, crystalline structure, and C/N ratio (of g-C_3N_4 structures) play an important role in photocatalytic CO_2 reduction using photocatalysts based on g-C_3N_4/TiO_2 nanocomposites (Ong *et al*., 2016).

Specific surface area is important since it could enhance CO_2 adsorption on the photocatalyst, making its photocatalytic reduction feasible. Moreover, the C/N ratio may allow controlling the g-C_3N_4 band gap energy, given that some authors have reported that materials with a high C/N ratio exhibit a band gap decrease. In addition, g-C_3N_4 materials with a low C/N ratio show a poor charge carrier separation and charge transport, both factors negatively affecting the photocatalytic activity (Ong *et al*., 2016). TiO_2 crystalline structure is another important characteristic to obtain g-C_3N_4/TiO_2 nanocomposites with high photocatalytic activity to reduce CO_2. It is well known that anatase TiO_2 presents the highest photocatalytic activity since its conduction band redox potential is suitable, so that CO_2 reduction can be a thermodynamically allowed reaction. Moreover, high crystallinity is also required to obtain TiO_2 materials with high electron/hole mobility. In most of the studies on g-C_3N_4/TiO_2 nanocomposites with high photocatalytic activity to produce solar fuels, anatase has been reported as the main TiO_2 crystalline structure.

There are just few studies about the use of g-C_3N_4/TiO_2 nanocomposites to photocatalytically reduce CO_2 in water (Acharya and Parida, 2020). For instance, Zhang *et al*. (2018) reported the synthesis of hollow g-C_3N_4/TiO_2 with high surface area and its evaluation in CO_2 photocatalytic assisted reduction under visible light irradiation. This nanocomposite showed an interesting methanol production due to an efficient charge separation occurring in the nanocomposite, probably due to a type II heterojunction.

Adekoya *et al*. (2017) found that modification of g-C_3N_4/TiO_2 with copper created islands of CuO and metal copper onto the nanocomposite surface, generating Schottky barriers (with metallic copper) and CuO acting as an electron trapping site for CO_2 adsorption, which enhanced the charge separation and charge transfer to CO_2. The main reduced products detected were methanol and formic acid. Wang *et al.* (2020) prepared g-C_3N_4/TiO_2 with direct Z-scheme containing gold nanoparticles. These materials showed an efficient production of light-induced electrons able to reduce CO_2 molecules into CH_4 and CO. The selectivity of CH_4 product was around 66%.

IV. CONCLUSIONS

Nanocomposites of g-C_3N_4/TiO_2 either as type II heterojunctions or direct z-scheme can overcome several drawbacks exhibited by TiO_2 and g-C_3N_4 separately, such as high electron-hole recombination, lack of visible light absorption, and low specific surface area.

These nanocomposites seem to be promising to be applied in photocatalytic reductive processes such as CO_2 in water interfaces and are an interesting strategy to help reduce greenhouse gases and produce solar fuels such as methanol.

ACKNOWLEDGEMENTS

Authors thank to National Scientific and Technical Research Council (CONICET) (Grant PIP 1492 and PIO 024), National University of La Plata (Grant X879) for their financial support and especially to R. Manrique-Holguín (ricardo.manrique@ucp.edu.co) for his contribution and support in image designing.

REFERENCES

Abdullah, H., Khan, M.M.R., Ong, H.R. and Yaakob, Z. (2017) Modified TiO_2 photocatalyst for CO_2 photocatalytic reduction: An overview. *J. CO_2 Utilization*. **22**, 15–32.

Acharya, R. and Parida, K. (2020) A review on TiO_2/g-C_3N_4 visible-light-responsive photocatalysts for sustainable energy generation and environmental remediation. *J. Environ. Chem. Eng.*. **8**, 103896.

Adekoya, D.O., Tahir, M. and Amin, N.A.S. (2017) g-C_3N_4/(Cu/TiO_2) nanocomposite for enhanced photoreduction of CO_2 to CH_3OH and HCOOH under UV/visible light. *J. CO_2 Utilization*. **18**, 261–274.

Banco Mundial (2022) *Emisiones de CO_2 (toneladas metricas per capita)*. https://datos.bancomundial.org/indicador/EN.ATM.CO2E.PC?view=chart (Accessed: 1 August 2022).

Dai, L., Xue, Y., Qu, L., Choi, H.-J. and Beak, J.-B. (2015) Metal-Free Catalysts for Oxygen Reduction Reaction. *Chem. Rev.*. **115**, 4823–4892.

Fujishima, A. and Honda, K. (1972) Electrochemical photolysis of water at a semiconductor electrode. *Nature*. **238**, 37–38.

Gong, E., Ali, S., Hiragond, C.B., Kin, H.S., Powar, N.S., Kim, D., Kim, H. and In S.-I. (2022) Solar fuels: research and development strategies. *Energy Environ. Sci.*. **15**, 880–939.

Inoue, T., Fujishima, A., Konishi, S. and Honda, K. (1979) Photoelectrocatalytic reduction of carbon dioxide in aqueous suspensions of semiconductor powders. *Nature*. **277,** 637–638.

Koci, K., Obalova, L., Matejova, L., Placha, D., Lacny, Z., Jirkovsky, J. and Solcova, O. (2009) Effect of TiO_2 particle size on the photocatalytic reduction of CO_2. *Appl. Catal. B.* **89**, 494–502.

Mohamed, H.H. and Bahnemann, D.W. (2012) The role of electron transfer in photocatalysis: Fact and fictions. *Appl. Catal. B.* **128**, 91–104.

Moser, J. and Gratzel, M. (1983) Light-Induced Electron Transfer in Colloidal Semiconductor Dispersions: Single vs. Dielectronic Reduction of Acceptors by Conduction-Band Electrons. *J. Am. Chem. Soc*. **105**, 6547–6555.

Nahar, S., Zain, M.F.M., Kadhum, A.A.H., Hasan, H.A. and Hasan, M.R. (2017) Advances in photocatalytic CO_2 reduction with water: A review. *Materials*. **10,** 10060629.

Ong, W.J., Tan, L.-L., Ng, Y.H., Yomg, S.-T. and Chai, S.-P. (2016) Graphitic Carbon Nitride (g-C_3N_4)-Based Photocatalysts for Artificial Photosynthesis and Environmental Remediation: Are We a Step Closer to Achieving Sustainability?. *Chem. Rev*. **116**, 7159–7329.

Osorio-Vargas, P., Pais-Ospinam D., Marín-Silva, D.A., Pinotti, A., Damonte, L., Cánneva, A., Donadelli, J.A., Pereira da Costa, L., Pizzio, L.R., Torres, C.C., Campos, C.H. and Rengifo-Herrera, J.A. (2022) TiO_2 nanorods doped with g-C_3N_4 – Polyethylene composite coating for self-cleaning applications. *Mater. Chem. Phys.* **288**, 126356.

Parrino, F. and Palmisano, L. (2021) *Titanium Dioxide (TiO_2) and Its Applications*. Edited by F. Parrino and L. Palmisano. Elsevier.

Pérez-Obando, J., Marín-Silva, D.A., Pinotti, A., Pizzio, L.R., Osorio-Vargas, P. and Rengifo-Herrera, J.A. (2019) Degradation study of malachite green on chitosan films containing heterojunctions of melon/TiO_2 absorbing visible-light in solid-gas interfaces. *Appl. Catal. B.* **244**, 773–785.

Qi, K., Cheng, B., Yu, J. and Ho, W. (2017) A review on TiO_2-based Z-scheme photocatalysts. *Cuihua Xuebao/Chinese J. Catal.* **38,** 1936–1955.

Remiro-Buenamañana, S. and García, H. (2019) Photoassisted CO_2 Conversion to Fuels. *ChemCatChem*. **9**, 342–356.

Rengifo-Herrera, J.A., Osorio-Vargas, P. and Pulgarin, C. (2022) A critical review on N-modified TiO_2 limits to treat chemical and biological contaminants in water. Evidence that enhanced visible light absorption does not lead to higher degradation rates under whole solar light. *J. Haz. Mater*. **425,** 127979.

Schneider, J., Matsuoka, M., Takeuchi, M., Zhang, J., Horiuchi, Y., Anpo, M. and Bahnemann, D.W. (2014) Understanding TiO_2 Photocatalysis: Mechanisms and Materials. *Chem. Rev*. **114**, 9919–9986.

Shehzad, N., Tahir, M., Johari, K., Murugesan, T. and Hussain, M. (2018) A critical review on TiO_2 based photocatalytic CO_2 reduction system: Strategies to improve efficiency. *J. CO_2 Utilization*. **26**, 98–122.

Tu, W., Zhou, Y. and Zou, Z. (2014) Photocatalytic conversion of CO_2 into renewable hydrocarbon fuels: State-of-the-art accomplishment, challenges, and prospects. *Adv. Mater*. **26**, 4607–4626.

US Environmental Protection Agency (2022) *Inventory of US Greenhouse Gas Emissions and Sinks*. Available at: https://www.epa.gov/ghgemissions/inventory-us-greenhouse-gas-emissions-and-sinks (Accessed: 1 August 2022).

Vu, N., Kaliaguine, S. and Do, T. (2019) Critical Aspects and Recent Advances in Structural Engineering of Photocatalysts for Sunlight-Driven Photocatalytic Reduction of CO_2 into Fuels. *Advanced func*. **29**, 1901825.

Wang, C., Zhao, Y., Xu, H., Li, Y., Wei, Y., Liu, J. and Zhao, Z. (2020) Efficient Z-scheme photocatalysts of ultrathin g-C_3N_4-wrapped Au/TiO_2-nanocrystals for enhanced visible-light-driven conversion of CO_2 with H_2O. *Appl. Catal. B.* **263**, 118314.

Wang, X., Maeda, K., Thomas, A., Takanabe, K, Xin, G., Carlsson, J.M., Domen, K. and Antonietti, M. (2009) A metal-free polymeric photocatalyst for hydrogen production from water under visible light. *Nature Mater*. **8**, 76–80.

Ward, M.D., White, J.R. and Bard, A.J. (1983) Electrochemical Investigation of the Energetics of Particulate Titanium Dioxide Photocatalysts. The Methyl Viologen-Acetate System. *J. Am. Chem. Soc.* **105**, 27–31.

Wen, J., Xie, J., Chen, X. and Li, X. (2017) A review on g-C_3N_4-based photocatalysts. *Appl. Surf. Sci.* **391**, 72–123.

Xie, S., Ma, W., Wu, X., Zhang, H., Zhang, Q., Wang, Y, and Wang, Y. (2021) Photocatalytic and electrocatalytic transformations of C1 molecules involving C-C coupling. *Energy Environ. Sci.* **14**, 37–89.

Yu, J., Wang, S., Low, J. and Xiao, W. (2013) Enhanced photocatalytic performance of direct Z-scheme g-C_3N_4-TiO_2 photocatalysts for the decomposition of formaldehyde in air. *Phys. Chem. Chem. Phys.* **15**, 16883–16890.

Zhang, L., Mohamed, H.H., Dillert, R. and Bahnermann, D. (2012) Kinetics and mechanisms of charge transfer processes in photocatalytic systems: A review. *J. Photochem. Photobio. C.* **13**, 263–276.

Zhang, L., Xie, C., Jiu, H., Meng, Y., Zhang, Q. and Gao, Y. (2018) Synthesized Hollow TiO_2@g-C_3N_4 Composites for Carbon dioxide Reduction Under Visible Light. *Catal. Letters*. **148**, 2812–2821.

Zhang, X., Chen, Y.L., Liu, R.-S. and Tsai, D.P. (2013) Plasmonic photocatalysis. *Rep. Prog. Phys.* **76,** 046401.

Received: August 29, 2022
Sent to Subject Editor: September 3, 2022
Accepted: December 13, 2022
Recommended by Subject Editor Laura Briand